

Organic Vapor Sorption in a High Surface Area Dysprosium(III)–Phosphine Oxide Coordination Material

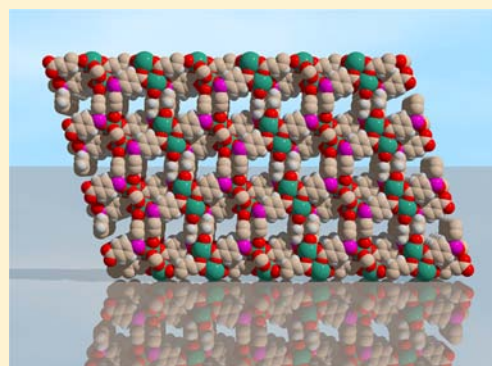
Ilich A. Ibarra,[†] Ji Woong Yoon,[‡] Jong-San Chang,[‡] Su Kyoung Lee,[‡] Vincent M. Lynch,[†] and Simon M. Humphrey^{*,†}

[†]Department of Chemistry and Biochemistry, The University of Texas at Austin, 1 University Station A5300, Austin, Texas 78712-0165, United States

[‡]Catalysis Center for Molecular Engineering, Korea Research Institute of Chemical Technology, P.O. Box 107, Yusong, Daejeon, 305-600, Korea

S Supporting Information

ABSTRACT: PCM-16 is a phosphine coordination material comprised of Dy(III) and triphenylphosphine oxide, which displays the highest reported CO₂ BET surface area for a Ln(III) coordination polymer of 1511 m² g⁻¹. PCM-16 also adsorbs 2.7 wt % H₂ and 65.1 wt % O₂ at 77 K and 0.97 bar. The adsorption–desorption behavior of a series of organic vapors has been studied in PCM-16 to probe the nature of certain host–guest interactions in the pores. Aromatic and polar guest species showed high uptakes and marked adsorption/desorption hysteresis, while aliphatic vapors were less easily adsorbed. The surface area of PCM-16 could be increased significantly (to 1814 m² g⁻¹) via exchange of Me₂NH₂⁺ cations in the pores with smaller NH₄⁺ groups.



■ INTRODUCTION

Porous coordination materials that incorporate esoteric organic substituents are currently of great interest because they may induce particular host–guest selectivity.¹ For example, inclusion of polar or charged organic groups in a coordination polymer may improve the adsorption enthalpy and/or spatial orientation of certain polarizable guest adsorbates such as CO₂.²

Phosphine ligands are ideally suited for construction of such materials because established P(III)/P(V) chemistry provides easy access to a variety of polar or ionic derivatives by reaction at the nucleophilic phosphine-*P*. Furthermore, phosphine-based coordination polymer building blocks can be modified both pre- or postsynthetically to provide unique routes to porous materials that are decorated with organic moieties that have not previously been studied in the realm of coordination polymer chemistry.^{3,4} Phosphines with three acid-functionalized aryl rings are examples of uncommon 3-connected organic building blocks that exhibit trigonal geometry and thus favor construction of 3-dimensional coordination networks, as opposed to lower-dimensional (layered) solids. This has been demonstrated by recent work, where tris(*p*-carboxylato)triphenylphosphine,^{5,6} its corresponding oxide,⁷ and also a methylphosphonium derivative^{5,8} have provided diverse examples of so-called phosphine coordination materials (PCMs).

A recent extension of this research has focused on preparation of lanthanide-based PCMs using tris(*p*-carboxylato)triphenylphosphine oxide,⁹ the polar P=O moiety favors direct coordination to Ln(III) cations in addition to Ln–

carboxylate bonds, so the phosphine oxide behaves as an asymmetric, 4-connected ligand that is tetrahedral at *P*. Porous coordination polymers constructed from lanthanide metals remain uncommon in comparison to the plethora of examples of d-block materials. This is perhaps due to the comparatively unpredictable variation in coordination numbers and geometries exhibited by f-block metals.¹⁰ Thus far, literature examples of lanthanide coordination polymers have been focused mostly on their magnetic¹¹ and photoluminescence properties.¹² Somewhat surprisingly, the gas and vapor adsorption properties of homometallic f-block coordination polymers have received less attention.^{13–25} Here, we report the low-temperature synthesis and solid-state properties of a Dy(III)-based PCM and present an in-depth study of its small molecule adsorption properties: these include high H₂ and O₂ sorption capacity and hysteretic adsorption/desorption of a number of organic vapors.

■ EXPERIMENTAL SECTION

Materials and Methods. 1,4-Dibromobenzene and PCl₃ (Aldrich), Dy(NO₃)₃·xH₂O (Alfa Aesar), and HCl and H₂O₂ (Fisher Scientific) were used as received. Tetrahydrofuran, *N,N*-dimethylformamide, diethyl ether, chloroform, and dichloromethane (Fisher Scientific) were purified by degassing followed by column distillation on an Innovative Technologies Inc. PureSolv system and stored on molecular sieves under dry N₂ prior to use. PCM-16 was synthesized

Received: July 1, 2012

Published: November 1, 2012

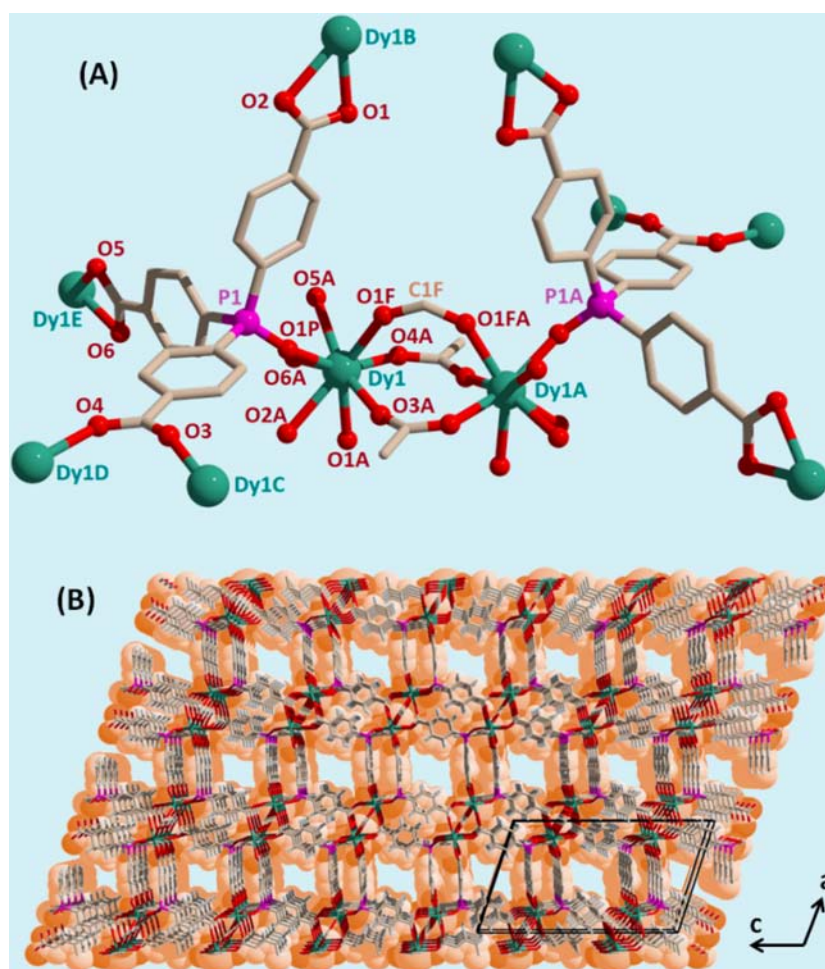


Figure 1. (A) Two asymmetric units of PCM-16 detailing the overall ligand connectivity and picturing a single three-quarter paddlewheel motif. (B) View of the open porous extended structure of PCM-16.

by heating mixtures in 40 capped scintillation vials using graphite thermal baths, with the vials submerged below the internal solvent level. Infrared spectra were collected on crystalline analyte using a Nicolet Avatar 330 FT-IR spectrometer fitted with attenuated total reflectance apparatus. Thermogravimetric analysis (TGA) was performed under a He atmosphere at a scan rate of $2.0\text{ }^{\circ}\text{C min}^{-1}$ in the range $25\text{--}800\text{ }^{\circ}\text{C}$ using a TA Instruments Q50 analyzer. NMR analyses, ^1H and ^{31}P , were recorded in house using a 300 MHz Oxford Instruments Cryomagnetic Systems spectrometer. Elemental microanalyses were performed by QTI Intertek, NJ.

Synthesis of Trilithium Salt of Tris(*p*-carboxylato)triphenylphosphine ($\{\text{P}(\text{C}_6\text{H}_4\text{-}p\text{-CO}_2\text{Li})_3\}$; tctpl_3). This ligand was prepared using the reported method,⁵ which is a modified version of the original procedure reported by Amengual et al.²⁶ that directly provides the trilithium salt. The salt was dried under vacuum to afford a pale yellow solid that was stored under N_2 (yield 68% based on the tris(*p*-bromo)triphenylphosphine intermediate). ^1H NMR (D_2O ; 300 MHz): $\delta = 7.38$ (t, 6H); 7.70 ppm (dd, 6H). ^{31}P NMR (D_2O ; 162 MHz): $\delta = -6.66$ ppm.

Synthesis of Tris(*p*-carboxylic)triphenylphosphine Oxide ($\{\text{P}(=\text{O})(\text{C}_6\text{H}_4\text{-}p\text{-CO}_2\text{H})_3\}$; tctpoH_3). Tctpl_3 (100 mg, 2.4 mmol) was dissolved into H_2O (10 cm^3) in a round-bottomed glass reactor tube fitted with a magnetic stir bar and heavy-duty Teflon-sealed screw cap. H_2O_2 (5 cm^3 , 30%) was added, and the mixture was vigorously stirred for 24 h. The resulting mixture was then cooled in an ice bath and acidified with ice cold HCl solution (1.0 M) to yield a white precipitate of tctpoH_3 that was isolated by vacuum filtration, washed with ether, and dried under vacuum (yield 614 mg, 63%). Anal. Calcd for $\text{C}_{21}\text{H}_{15}\text{O}_7\text{P}\cdot 2\text{H}_2\text{O}$: C, 56.5; H, 4.29. Found: C, 56.8; H, 3.94. ν_{max}

($\text{solid}/\text{cm}^{-1}$): 2929 w, 1699 m br, 1652 m, 1565 w, 1395 m, 1262 m br, 1161 m, 1103 s, 1017 m, 962 s, 933 s, 894 br s, 704 m. ^1H NMR (dms; 300 MHz): $\delta = 7.92$ (d, 6H), 8.15 (d, 6H) ppm. ^{31}P NMR (dms; 300 MHz): $\delta = 26.0$ ppm.

Synthesis of PCM-16 $[\text{Me}_2\text{NH}_2]\text{-}[\text{Dy}_2(\text{tctpo})_2(\text{O}_2\text{CH})]\cdot 3\text{dmf}\cdot 3\text{H}_2\text{O}$. tctpoH_3 (20 mg, 48 μmol) and $\text{Dy}(\text{NO}_3)_3\cdot x\text{H}_2\text{O}$ (65 mg, 186 μmol) were mixed in dmf (3.0 cm^3), thf (4.0 cm^3), H_2O (1.0 cm^3), and HCl (36.5%, 1 drop); the resulting pH of the mixture was 2.0. The slurry was stirred until complete dissolution occurred. The solution was then heated in a scintillation vial at $85\text{ }^{\circ}\text{C}$ in a graphite thermal bath for 4 days to yield colorless rods of the target material, which were isolated by decanting away any residual amorphous solid with the mother liquor (yield 23.0 mg, 64%). The same synthetic procedure was repeated in which HCl was substituted for formic acid (HCO_2H) to give pH = 2.0, which similarly afforded 23.7 mg, 66%. Anal. Calcd for $\text{C}_{54}\text{H}_{60}\text{Dy}_2\text{N}_4\text{O}_{22}\text{P}_2$: C, 43.12; H, 4.02; N, 3.73. Found: C, 43.33; H, 4.04; N, 3.74. ν_{max} ($\text{solid}/\text{cm}^{-1}$): 3662 w, 3587 m, 2896 s, 2784 m, 2482 m, 2325 m, 1729 br m, 1465 w, 1377 s, 1276 m, 1156 s, 1079 s, 857 w, 756 m, 719 s.

Preparation of NH_4^+ Exchanged PCM-16 $[\text{NH}_4]\text{-}[\text{Dy}_2(\text{tctpo})_2(\text{O}_2\text{CH})]\cdot 2\text{dmf}\cdot 3\text{H}_2\text{O}$. A NH_4^+ -exchanged sample in which Me_2NH_2^+ was replaced by NH_4^+ was prepared by immersing crystals of as-synthesized PCM-16 in a saturated solution of NH_4Cl predissolved in a mixture of dmf (3.0 cm^3), thf (4.0 cm^3), and H_2O (3.0 cm^3). Crystals were soaked for 4 days, during which time the NH_4Cl solution was refreshed three times per day. After decanting away the NH_4Cl solution, the cation-exchanged crystals of PCM-16- NH_4^+ were rinsed and soaked in a mixture of dmf (3.0 cm^3), thf (4.0 cm^3), and H_2O (3.0 cm^3) for 1 day, repeatedly, to remove residual free

NH₄Cl. Anal. Calcd for C₄₉H₄₉Dy₂N₃O₂₁P₂: C, 41.95; H, 3.52; N, 3.00. Found: C, 41.87; H, 3.58; N, 3.02. ν_{max} (solid/cm⁻¹): 3696 w, 3575 m, 2897 s, 2784 m, 2465 m, 2316 m, 1721 br m, 1471 w, 1379 s, 1256 m, 1165 s, 868 w, 761 m, 714 s.

Single-Crystal X-ray Diffraction. Crystals were mounted on thin fiber loops using perfluoropolyether oil, which was frozen in situ by a nitrogen gas Cryostream flow. Data for PCM-16 was collected on a Rigaku AFC-12 diffractometer fitted with a Saturn 724+ CCD detector using monochromated Mo K α radiation ($\lambda = 0.71075 \text{ \AA}$). Cell refinement and data reduction were performed using the CrystalClear²⁷ utility. Absorption corrections were made based on multiple ω scans using the SADABS²⁸ program. Structures were solved using direct methods and refined on F^2 using the program SIR-97²⁹ and then refined using SHELXTL-97³⁰ software. All non-hydrogen atoms were refined anisotropically for all atoms in the framework of PCM-16; uncoordinated dmf and H₂O solvent molecules were refined with isotropic displacement parameters. dmf molecules were refined with geometric restraints in order to stabilize the refinement process, and free variables were initially applied to determine the site occupancies of all solvent atoms, which were then set to 1.0 or 0.5 in the final refinement cycle. The Squeeze³¹ utility in PLATON³² was applied to the solution postrefinement in order to remove residual peaks due to remaining disordered solvent. This resulted in only small improvements to the final statistics (see CIF). All hydrogen atoms were fixed based on idealized coordinates and refined with U_{iso} values set to 1.5 times that of the carrier atom. Solvent H₂O H atoms were not directly located in the peak difference map; compensatory alterations were made to finalize the structural formula in the CIF to account for solvent H atoms that were not directly located in the electron peak difference map. See Supporting Information for full data in CIF format.

Crystal Data for PCM-16. C_{21.5}H_{12.5}DyO₈P; MW = 592.29, monoclinic, space group $P2_1/c$, $a = 14.537(3) \text{ \AA}$, $b = 10.492(2) \text{ \AA}$, $c = 23.403(5) \text{ \AA}$, $\beta = 107.32(3)^\circ$, $V = 3407.8(12) \text{ \AA}^3$, $Z = 4$, $\rho = 1.154 \text{ g cm}^{-3}$, $\mu(\text{Mo K}\alpha) = 2.268 \text{ mm}^{-1}$, $R_1 = 0.057$, 49 072 measured reflections (5990 independent reflections, $I > 2\sigma(I)$), $wR_2 = 0.146$ (all data), $R_{\text{int}} = 0.124$, GoF = 1.03; CCDC 883819.

Powder X-ray Diffraction. Phase purity and thermal stability of PCM-16 were confirmed by analysis of powdered crystalline samples that were sealed inside borosilicate capillary tubes under inert atmosphere conditions and spun in situ to prevent preferential orientation of the crystallites. Diffractograms were recorded on a Rigaku Spider diffractometer equipped with an image plate detector, operating in Debye–Scherrer geometry using Cu K α radiation (1.5412 \AA). The 2-dimensional image plate data was converted to give a 1-dimensional pattern using Rigaku Corp. 2DP software.³³ Reflection data in the range 5.0–35.0° 2θ was extracted from the entire data set. The PXRD patterns were then compared directly to their corresponding simulated patterns that were generated using the *SimPowPatt* facility in Platon³² using *hkl* reflection data obtained from the single-crystal experiment.

Gas Adsorption Isotherms. CO₂, N₂, O₂, Ar, and H₂ isotherms were recorded on an Autosorb-I system (Quantachrome) at The University of Texas at Austin under ultrahigh vacuum in a clean system with a diaphragm and turbo pumping system. Ultrahigh purity ($\geq 99.9995\%$) CO₂, N₂, O₂, Ar, and H₂ were purchased from Praxair. The surface area was calculated using the BET method based on adsorption data in the partial pressure (p/p_0) range 0.05–0.30 for CO₂ and N₂.

RESULTS AND DISCUSSION

The 3-dimensional porous coordination polymer [Me₂NH₂]-[Dy₂(tctpo)₂(O₂CH)]·3dmf·3H₂O (PCM-16) is comprised of a single phosphine oxide trianion, [P(=O)(C₆H₄-4-CO₂)₃]³⁻ (tctpo), that is multiply coordinated by a single Dy(III) center (Figure 1A). Each Dy(III) has a distorted square antiprismatic coordination sphere that consists of carboxylate donors (chelating and bridging) and a single P=O–Dy bond (Figure 1A). These account for seven interactions; the eighth is

provided by a formate anion (O1F–C1F–O1FA) that bridges two adjacent Dy(III) ions. The presence of formate in the structure is explained by acid-catalyzed hydrolysis of *N,N*-dimethylformamide solvent. PCM-16 could be synthesized in high yield (64–66%) either using a small amount of HCl to drive the hydrolysis reaction in situ or by direct addition of formic acid to the reaction mixture. The resulting Dy dimers in PCM-16 are essentially three-quarter paddlewheel motifs with a single formate bridge perpendicular to the carboxylate bridges. The formate ligand necessitates charge balance by a single cation per formula unit. An obvious cation was not located in the single-crystal structure. It is most likely that the cation is a delocalized Me₂NH₂⁺ resident on solvent within the channel or on the framework itself.^{7a} PCM-16 has infinite 3-dimensional connectivity with quadrilateral pore windows in all three crystallographic planes (Figure 1B and Supporting Information), the largest of which have accessible corner-to-corner openings of 11.8 \AA . As is expected for network solids constructed using high-coordinate metals and unusual 3-dimensional ligands, PCM-16 has a convoluted net topology in which the metal and phosphine oxide both act as 5-c nodes, in addition to the 2-c formate bridge (Supporting Information Figure S2). Microwave-assisted synthesis and X-ray crystal structures of a related family of materials of formula [Me₂NH₂][Ln₂(tctpo)₂(O₂CH)]·4dmf·6H₂O (Ln = Sm–Lu) with a network topology that is isostructural to PCM-16 were reported recently;^{9b} however, no solid-state analysis was performed on the Dy-based material.

Thermogravimetric analysis (TGA) of a crystalline sample of PCM-16 showed a continual mass loss of 21.1 wt % in the range 25–200 °C, which, supported by microanalytical data, corresponds closely to the calculated value for 3 dmf and 3 H₂O molecules per formula unit (20.0 wt %) (Supporting Information Figure S3). The fully desolvated material remained stable up to 440 °C. In situ variable-temperature powder X-ray diffraction (PXRD) of PCM-16 under vacuum (1×10^{-10} bar) confirmed retention of framework crystallinity at 150 °C. Above 200 °C and under vacuum, a phase transition was observed to a new crystalline phase that was stable up to 350 °C (Supporting Information Figure S4). Although it was not possible to ascertain the absolute structure of this new phase via single-crystal X-ray diffraction, the original low-temperature PXRD pattern corresponding to PCM-16 was easily recovered by exposure of the material to humid air (see Supporting Information Figure S5). On the basis of this observation, all subsequent textural measurements of PCM-16 were performed on crystalline samples that were activated below the phase transition temperature.

Primary assessment of the surface area of an activated sample of PCM-16 (150 °C, 1×10^{-10} bar, 12 h) using N₂ and CO₂ probe gases gave BET surface areas of 620 and 1511 m² g⁻¹, respectively (Figure 2); the estimated CO₂ micropore volume for PCM-16 was 0.83 cm³ g⁻¹. The disparity in the observed BET surface areas suggested that PCM-16 has a significantly greater affinity for CO₂ adsorption, as has been previously reported for other porous f-block coordination polymers.¹³ The measured surface area of PCM-16 surpasses the recently reported Tb(III)-based material (PCM-15) which showed the highest CO₂ surface area (1187 m² g⁻¹) reported to date for an f-block porous coordination polymer.^{9a} The lower N₂ BET surface area is similar to other important recent examples of Ln(III)-based porous coordination polymers, such as Tb(btc) (678 m² g⁻¹),²⁰ the PCN-17 series (Er, 606 m² g⁻¹; Dy, 738 m²

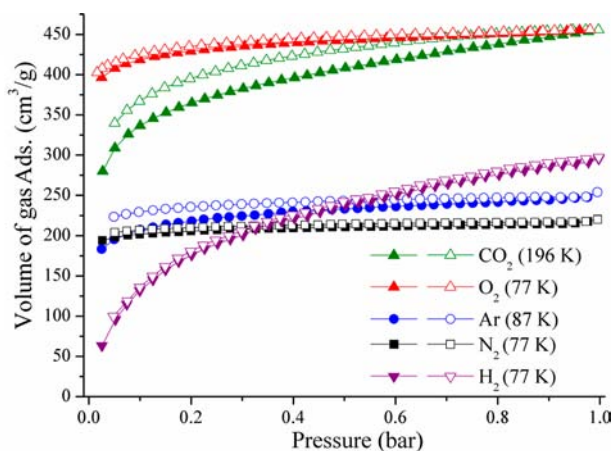


Figure 2. Observed type-I adsorption/desorption isotherms for PCM-16.

g^{-1} ; Yb, $820 \text{ m}^2 \text{ g}^{-1}$,^{22,23} or Tb(btb)(OH₂) ($730\text{--}930 \text{ m}^2 \text{ g}^{-1}$).¹⁷ Due to the apparent preference of PCM-16 to adsorb CO₂ over N₂, the isosteric heat of adsorption of CO₂ was derived from adsorption studies conducted at 278 and 298 K. Fitting of both isotherms to a virial-type equation³⁴ gave an estimated value of 35.7 kJ mol^{-1} (Supporting Information Figures S8 and S14). Kaneko et al. previously reported a heat of adsorption for CO₂ of $30.10 \text{ kJ mol}^{-1}$ for Er₂(pda)₃.¹⁵

Following confirmation of the inherent porosity of PCM-16, adsorption experiments using alternative probe analytes were carried out on fresh, desolvated samples. H₂ sorption studies at 77 K revealed rapid uptake kinetics and reversibility without hysteresis (Figure 2; purple triangles). Total H₂ uptake was 2.66 wt % at 77 K and $p/p_0 = 1.0$ ($295.61 \text{ cm}^3 \text{ g}^{-1}$, 26.60 mg g^{-1}). This uptake is also significantly higher than the previously highest reported H₂ uptake for a Ln(III)-based coordination polymer (1.96 wt %).^{9a} The isosteric heat of adsorption of H₂ in PCM-16 was estimated as 8.1 kJ mol^{-1} using data at 77 and 87 K (see Supporting Information Figure S7 and Figure S13). Hong et al. previously reported a value of 7.8 kJ mol^{-1} for Gd(tcipo).¹³ O₂ adsorption at 77 K showed a total uptake of $456 \text{ cm}^3 \text{ g}^{-1}$ ($65.1 \text{ wt} \%$ at 0.97 bar; Figure 2, red triangles). Total Ar uptake was measured as $254 \text{ cm}^3 \text{ g}^{-1}$ (Figure 2, blue circles).

A single cation is required in PCM-16 per formula unit to achieve overall charge balance. The identity of this cation was initially unclear to us, particularly in the desolvated (activated) form of PCM-16, in which vapor sorption analyses were performed. It is reasonable to assume that Me₂NH₂⁺ could be formed due to hydrolysis of dmf that also gave the formate anion which was incorporated into the framework of PCM-16. In previous work, ex situ ¹H NMR studies of the framework postdigestion in DCl revealed a peak that was attributed to Me₂NH₂⁺.^{9b} This study did not unequivocally determine the location of H⁺ species in the activated material, while it seemed plausible that H⁺ could move to several alternative locations in the framework upon heating under vacuum. To test this hypothesis from an alternative route, we decided to attempt cation exchange of the as-synthesized PCM-16.³⁵

A sample of PCM-16 was subjected to cation exchange using a saturated solution of NH₄Cl in solvent of synthesis (see Experimental Section), and the surface area of the resulting material was studied by CO₂ sorption analysis in addition to other characterization studies. Thus, NH₄-PCM-16 was

prepared and activated at 150 °C and 1×10^{-10} bar for 12 h. Interestingly, the CO₂ gas adsorption experiment at 196 K gave a BET surface area of $1814 \text{ m}^2 \text{ g}^{-1}$ (Supporting Information Figure S15), which is 17% higher than the as-synthesized PCM-16. Schröder et al. previously showed that replacement of Me₂NH₂⁺ by smaller Li⁺ cations enhanced the porosity of a MOF-type material by ca. 25%.³⁵ Thus, it seems very likely in this instance that the observed increase of surface area was indeed due to replacement of larger Me₂NH₂⁺ groups by smaller NH₄⁺. Successful exchange of cations inside PCM-16 using the method employed herein was confirmed by elemental and TGA analyses (Supporting Information Figure S16).

Selective vapor sorption at ambient temperature by highly porous coordination polymers is an interesting and largely unexplored potential application.²⁵ Since PCM-16 appeared to be an ideal candidate, the uptake of benzene, toluene, ethanol (Figure 3), *n*-hexane, and cyclohexane (Figure 4) were all

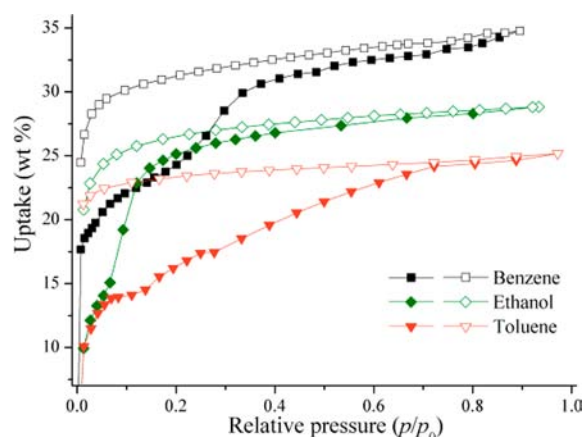


Figure 3. Observed adsorption-desorption isotherms for benzene, toluene, and ethanol vapors in PCM-16 at 298 K. Solid symbols represent adsorption, and open symbols show desorption.

studied. These analytes were specifically chosen to allow for a comparative analysis of preferential host-guest interactions within the pores. First, the relative hydrophilicity/hydrophobicity of PCM-16 was probed by vapor sorption of apolar aromatics versus ethanol (Figure 3). Benzene, toluene, and

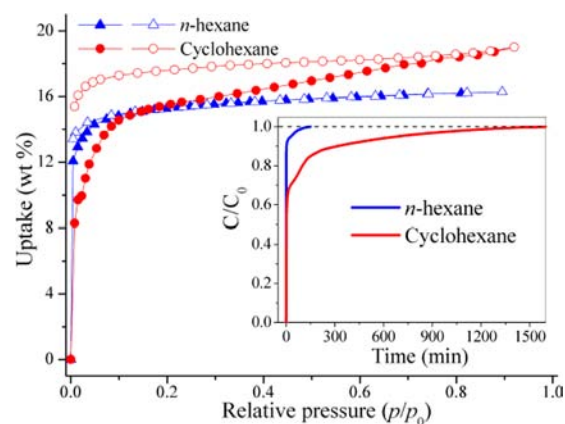


Figure 4. Adsorption-desorption isotherms for *n*-hexane and cyclohexane in PCM-16 at 298 K; solid symbols represent adsorption, and open symbols show desorption. (Inset) Corresponding time-dependence plot.

ethanol each underwent rapid uptake at low pressure, leading to saturation below $p/p_0 = 0.2$, indicative of favorable host–guest interactions in all cases. The internal pore surfaces of PCM-16 are comprised primarily of aromatic rings, so it is not difficult to understand why the aromatic vapors would be easily adsorbed via π – π interactions. Polar species such as ethanol most likely form hydrogen-bonded interactions with the charged moieties (Dy–carboxylates in this instance). The highest vapor uptake in PCM-16 was observed for benzene (34.8 wt % or 10.5 molecules per unit cell; Supporting Information Figure S17). Toluene showed a lower total uptake, as expected due to the larger adsorbate size (25.2 wt %, kinetic diameter = 5.9 Å; 6.5 molecules per unit cell; Figure 3, orange triangles). While there are no examples of analogous vapor adsorption studies in other Ln-based porous coordination polymers, the present data can be contrasted against similar measurements on d-metal-based polymers, such as Ni(bpb) (bpb = 1,4-bis(4-tetrazolyl)-benzene) which exhibited a benzene uptake of 5.8 mmol g⁻¹, corresponding to 45.3 wt % under comparable conditions.³⁶ The higher wt % uptake observed in the latter case is to be expected, since the density of the Ni-based material is significantly lower than the Dy-based PCM-16.

Ethanol adsorption in PCM-16 exhibited an uptake of 28.8 wt % (15 molecules per unit cell). Strong hysteresis was observed for all three probe molecules, with marked stepped profiles in the desorption phase (Figure 3, open symbols). The largest pore openings in PCM-16 are significantly larger than the kinetic diameters of the adsorbates (toluene, 5.9 Å; benzene, 5.8 Å; ethanol, 4.5 Å).²⁵ Therefore, it does not seem appropriate to invoke ‘kinetic trap’ arguments that have been suggested by others.³⁷ Instead, the observed hysteresis is likely due to moderately strong host–guest interactions, which result in physical ‘sticking’ of the guests within the pores.

In an additional study to support this hypothesis, the kinetic sorption of the apolar aliphatic species cyclohexane and *n*-hexane was studied (Figure 4). The former showed a 19.0 wt % uptake (5.3 molecules per unit cell; Supporting Information Figure S18), while 16.3 wt % (4.5 molecules per unit cell) of *n*-hexane was adsorbed at 298 K in PCM-16. A similar alkane vapor adsorption study was made on the Cr-based MIL-53, in which Trens and co-workers reported adsorption of 5.3 molecules of *n*-hexane per unit cell at 1 bar and 313 K.³⁸ In comparison to the former adsorbates, the aliphatics should be less likely to engage in substantial host–guest bonding interactions; this explains their comparatively lower uptakes. Most notably, however, the lack of any pronounced desorption hysteresis for the alkanes is consistent with the lack of strong host–guest interactions. Kinetic analysis of the aliphatic C₆ adsorbates showed that although the total uptakes were similar, the sorption rate of *n*-hexane was much faster than for cyclohexane (Figure 4, inset), which may be an effect of the disparity in kinetic diameters (4.3, 6.0 Å respectively).³⁹

CONCLUSION

The high surface area Dy(III)–phosphine oxide coordination polymer, PCM-16, has permitted an assessment of how coordination polymer materials could be employed in the sorption of certain organic vapors at ambient temperature. It is clear that sorption of aromatic and polar organic adsorbates inside PCM-16 was most favorable. In addition, their associated desorption kinetics were slow, due to the existence of favorable host–guest interactions within the pores, such as π – π bonding or weak dative contacts. In contrast, apolar aliphatic adsorbates

were only weakly bound inside PCM-16 and showed no marked desorption hysteresis. However, chemically similar adsorbates that have significantly different kinetic diameters (e.g., *n*-hexane and cyclohexane) could still be discriminated from one another, based on significantly different adsorption rates through the pore windows in PCM-16.

ASSOCIATED CONTENT

Supporting Information

Additional structural pictures, thermogravimetric analysis, PXRD patterns, derivation of the isosteric heats of adsorption for H₂ and CO₂, and solvent vapor adsorptions for PCM-16. This material is available free of charge via the Internet at <http://pubs.acs.org>.

AUTHOR INFORMATION

Corresponding Author

*E-mail: smh@cm.utexas.edu.

Notes

The authors declare no competing financial interest.

ACKNOWLEDGMENTS

The authors thank the Welch Foundation (F-1738) and the Institutional Research Program (ISTK, KK-1201-F0) for financial support and the National Science Foundation (Grant No. 0741973) for X-ray equipment.

REFERENCES

- (1) (a) Burrows, A. D. *CrysEngComm*. **2011**, *13*, 3623. (b) Murray, L. J.; Dincă, M.; Long, J. R. *Chem. Soc. Rev.* **2009**, *38*, 1294. (c) Dugan, E.; Wang, Z.; Okamura, M.; Medina, A.; Cohen, S. M. *Chem. Commun.* **2008**, 3366. (d) Yang, S.; Lin, X.; Blake, A. J.; Walker, G. S.; Hubberstey, P.; Champness, N. R.; Schröder, M. *Nat. Chem.* **2009**, *1*, 487. (e) Kasinathan, P.; Seo, Y.-K.; Shim, K.-E.; Hwang, Y. K.; Lee, U.-H.; Hwang, D. W.; Hong, D.-Y.; Halligudi, S. B.; Chang, J.-S. *Bull. Korean Chem. Soc.* **2011**, *32*, 2073.
- (2) (a) Lin, X.; Champness, N. R.; Schröder, M. *Top. Curr. Chem.* **2010**, *293*, 35. (b) Seo, J.; Jin, N.; Chun, H. *Inorg. Chem.* **2010**, *49*, 10833. (c) Shimomura, S.; Higuchi, M.; Matsuda, R.; Yoneda, K.; Hijikata, Y.; Kubota, Y.; Mita, Y.; Kim, J.; Takata, M.; Kitagawa, S. *Nat. Chem.* **2010**, *2*, 633. (d) Demessence, A.; Long, J. R. *Chem.—Eur. J.* **2010**, *16*, 5902. (d1) Yang, S.; Lin, X.; Lewis, W.; Suetin, M.; Bichoutskaia, E.; Parker, J. E.; Tang, C. C.; Allan, D. R.; Rizkallah, P. J.; Hubberstey, P.; Champness, N. R.; Thomas, K. M.; Blake, A. J.; Schröder, M. *Nat. Chem.* **2012**, *11*, 710. (e) Yang, S.; Sun, J.; Ramirez-Cuesta, A. J.; Callear, S. K.; David, W. I. F.; Anderson, D. P.; Newby, R.; Blake, A. J.; Parker, J. E.; Tang, C. C.; Schröder, M. *Nat. Chem.*, **2012**, DOI:10.1038/nchem.1457.
- (3) (a) Xu, X.; Nieuwenhuysen, M.; James, S. L. *Angew. Chem., Int. Ed.* **2002**, *41*, 764. (b) Plater, M. J.; Foreman, M. R. St. J.; Skakle, J. M. S. *J. Chem. Cryst.* **2000**, *30*, 499. (c) Plater, M. J.; Foreman, M. R. St. J.; Coronado, E.; Gómez-García, C. J.; Slawin, A. M. Z. *J. Chem. Soc., Dalton Trans.* **1999**, 4209.
- (4) McEwen, W. E.; Maier, L.; Miller, B. *Topics in Phosphorus Chemistry*; Grayson, M.; Griffith, E. J., Eds.; Wiley: New York, 1965; Vols. 1–2.
- (5) Humphrey, S. M.; Allan, P. K.; Oungoulian, S. E.; Ironside, M. S.; Wise, E. R. *Dalton Trans.* **2009**, 2298.
- (6) Nuñez, A. J.; Shear, L. N.; Dahal, N.; Ibarra, I. A.; Yoon, J. W.; Hwang, Y. K.; Chang, J.-S.; Humphrey, S. M. *Chem. Commun.* **2011**, 47, 11855.
- (7) (a) Humphrey, S. M.; Oungoulian, S. E.; Yoon, J. W.; Hwang, Y. K.; Wise, E. R.; Chang, J.-S. *Chem. Commun.* **2008**, 2891. (b) Bohnsack, A. M.; Ibarra, I. A.; Hatfield, P. W.; Yoon, J. W.; Hwang, Y. K.; Chang, J.-S.; Humphrey, S. M. *Chem. Commun.* **2011**, 47, 4899.

- (8) Ibarra, I. A.; Tan, K. E.; Lynch, V. M.; Humphrey, S. M. *Dalton Trans.* **2012**, *41*, 3920.
- (9) (a) Ibarra, I. A.; Hesterberg, T. W.; Holliday, B. J.; Lynch, V. M.; Humphrey, S. M. *Dalton Trans.* **2012**, *41*, 8003. (b) Lin, Z.-J.; Yang, Z.; Liu, T.-F.; Huang, Y.-B.; Cao, R. *Inorg. Chem.* **2012**, *51*, 1813.
- (10) See, for example: (a) Zhao, B.; Cheng, X.-Y.; Cheng, P.; Liao, D.-Z.; Yan, S.-P.; Jiang, Z.-H. *J. Am. Chem. Soc.* **2004**, *126*, 15394. (b) Plabst, M.; Bein, T. *Inorg. Chem.* **2009**, *48*, 4331. (c) Long, D.-L.; Blake, A. J.; Champness, N. R.; Wilson, C.; Schröder, M. *J. Am. Chem. Soc.* **2001**, *123*, 3401.
- (11) (a) Tanase, S.; Reedijk, J. *Coord. Chem. Rev.* **2006**, *250*, 2501. (b) Huang, Y.-G.; Jiang, F.-L.; Hong, M.-C. *Coord. Chem. Rev.* **2009**, *253*, 2814. (c) Hong, M. *Cryst. Growth Des.* **2007**, *7*, 10.
- (12) See for example: (a) Falcario, P.; Furukawa, S. *Angew. Chem., Int. Ed.* **2012**, *51*, 8431. (b) Yang, X.; Jones, R. A. *J. Am. Chem. Soc.* **2005**, *127*, 7686. (c) Yang, X.; Hahn, B. P.; Jones, R. A.; Stevenson, K. J.; Swinnea, J. S.; Wu, Q. *Chem. Commun.* **2006**, 3827. (d) Ma, L.; Evans, O. R.; Foxman, B. M.; Lin, W. *Inorg. Chem.* **1999**, *38*, 5837.
- (13) Lee, W. R.; Ryu, D. W.; Lee, J. W.; Yoon, J. H.; Koh, E. K.; Hong, C. S. *Inorg. Chem.* **2010**, *49*, 4723.
- (14) Reineke, T. M.; Eddaoudi, M.; O'Keeffe, M.; Yaghi, O. M. *Angew. Chem., Int. Ed.* **1999**, *38*, 2590.
- (15) Pan, L.; Adams, K. M.; Hernandez, H. E.; Wang, X.; Zheng, C.; Hattori, Y.; Kaneko, K. *J. Am. Chem. Soc.* **2003**, *125*, 3062.
- (16) Rosi, N. L.; Kim, J.; Eddaoudi, M.; Chen, B.; O'Keeffe, M.; Yaghi, O. M. *J. Am. Chem. Soc.* **2005**, *127*, 1504.
- (17) Devic, T.; Serre, C.; Audegrand, N.; Marrot, J.; Férey, G. *J. Am. Chem. Soc.* **2005**, *127*, 12788.
- (18) Devic, T.; Wagner, V.; Guillou, N.; Vimont, A.; Haouas, M.; Pascolini, M.; Serre, C.; Marrot, J.; Daturi, M.; Taulelle, F.; Férey, G. *Microporous Mesoporous Mater.* **2011**, *140*, 25.
- (19) Jia, J.; Lin, X.; Blake, A. J.; Champness, N. R.; Hubberstey, P.; Shao, L.; Walker, G.; Wilson, C.; Schröder, M. *Inorg. Chem.* **2006**, *45*, 8838.
- (20) Khan, N. A.; Haque, Md. M.; Jhung, S. H. *Eur. J. Inorg. Chem.* **2010**, 4975.
- (21) Wang, G.; Song, T.; Fan, Y.; Xu, J.; Wang, M.; Wang, L.; Zhang, L.; Wang, L. *Inorg. Chem. Commun.* **2010**, *13*, 95.
- (22) Ma, S.; Wang, X.-S.; Yuan, D.; Zhou, H.-C. *Angew. Chem., Int. Ed.* **2008**, *47*, 4130.
- (23) Ma, S.; Yuan, D.; Wang, X.-S.; Zhou, H.-C. *Inorg. Chem.* **2009**, *48*, 2072.
- (24) Jiang, H.-L.; Tsumori, N.; Xu, Q. *Inorg. Chem.* **2010**, *49*, 10001.
- (25) Sun, J.-K.; Yao, Q.-X.; Tian, Y.-Y.; Wu, L.; Zhu, G.-S.; Chen, R.-P.; Zhang, J. *Chem.—Eur. J.* **2012**, *18*, 1924.
- (26) Amengual, R.; Genin, F.; Michelet, V.; Savignac, M.; Genêt, J.-P. *Adv. Synth. Catal.* **2002**, *344*, 393.
- (27) *CrystalClear, Automated data collection and processing suite*; Rigaku Americas Inc.: The Woodlands, TX, 2008.
- (28) *SADABS Area-Detector Absorption Correction*; Siement Industrial Automation, Inc.: Madison, WI, 1996.
- (29) Altamore, A.; Burla, M. C.; Camalli, M.; Cascarano, G. L.; Giacovazzo, C.; Guagliardi, A.; Moliterni, A. G. G.; Polidori, G.; Spagna, R. *SIR-97. J. Appl. Crystallogr.*, **1999**, *32*, 115.
- (30) Sheldrick, G. M. *SHELXTL-97. Acta Crystallogr.* **2008**, *A64*, 112.
- (31) van der Sluis, P.; Spek, A. L. *Acta Crystallogr.* **1990**, *A46*, 194.
- (32) Spek, A. L. *Platon, a Multipurpose Crystallographic Tool*; Utrecht University: Utrecht, The Netherlands, 2009.
- (33) *2DP, V. 1.0 Program for converting 2-Dimensional Area Detector Data to 1-Dimensional Powder Diffraction Data*; Rigaku Americas, Inc.: The Woodlands, TX, 2007.
- (34) (a) Czepirski, L.; Jagiello, J.; *Chem. Eng. Sci.* **1989**, *44*, 797. (b) Anson, A.; Jagiello, J.; Parra, J. B.; Sanjuan, M. L.; Benito, A. M.; Maser, W. K.; Martinez, M. T. *J. Phys. Chem. B* **2004**, *108*, 15820. (c) Okoye, I. P.; Benham, M.; Thomas, K. M. *Langmuir* **1997**, *13*, 4054. (d) Reid, C. R.; Thomas, K. M. *Langmuir* **1999**, *15*, 3206. (e) Reid, C. R.; Thomas, K. M. *J. Phys. Chem. B* **2001**, *105*, 10619. (f) Lin, X.; Telepeni, I.; Blake, A. J.; Dailly, A.; Brown, C. M.; Simmons, J. M.; Zoppi, M.; Walker, G. S.; Thomas, K. M.; Mays, T. J.; Hubberstey, P.; Champness, N. R.; Schröder, M. *J. Am. Chem. Soc.* **2009**, *131*, 2159.
- (35) Yang, S.; Lin, X.; Blake, A. J.; Thomas, K. M.; Hubberstey, P.; Champness, N. R.; Schröder, M. *Chem. Commun.* **2008**, 6108.
- (36) Galli, S.; Masciocchi, N.; Colombo, V.; Maspero, A.; Palmisano, G.; López-Garzón, F. J.; Domingo-García, M.; Fernández-Morales, I.; Barea, E.; Navarro, J. A. R. *Chem. Mater.* **2010**, *22*, 1664.
- (37) (a) Zhao, X. B.; Xiao, B.; Fletcher, A. J.; Thomas, K. M.; Bradshaw, D.; Rosseinsky, M. J. *Science* **2004**, *306*, 1012. (b) Choi, H. J.; Dincă, M.; Long, J. R. *J. Am. Chem. Soc.* **2008**, *130*, 7848.
- (38) Trung, T. K.; Trens, P.; Tanchoux, N.; Bourrelly, S.; Llewellyn, P. L.; Loera-Serna, S.; Serre, C.; Loiseau, T.; Fajula, F.; Férey, G. *J. Am. Chem. Soc.* **2008**, *130*, 16926.
- (39) Breck, D. W. *Zeolite Molecular Sieves: Structure, Chemistry and Use*; Wiley: New York, 1973.